Molecular Crystals and Liquid Crystals Science and Technology. Section A. Molecular Crystals and Liquid Crystals

Publication details, including instructions for authors and subscription information:
http://www.tandfonline.com/loi/gmcl19

Interpretation for STM Imaging of One-Dimensional Organic Conductors

N. Ara-kato [a], M. Kara [a], H. Sasabe [a] & W. Knoll [a]

[a] Frontier Research Program, RIKEN, Wako, Saitama, 351-01, Japan

Version of record first published: 04 Oct 2006.

To cite this article: N. Ara-kato , M. Kara , H. Sasabe & W. Knoll (1996): Interpretation for STM Imaging of One-Dimensional Organic Conductors, Molecular Crystals and Liquid Crystals Science and Technology. Section A. Molecular Crystals and Liquid Crystals, 280:1, 211-216

To link to this article: http://dx.doi.org/10.1080/10587259608040334

Mol. Cryst. Liq. Cryst., 1996, Vol. 280, pp. 211–216
Reprints available directly from the publisher
Photocopying permitted by license only

INTERPRETATION FOR STM IMAGING OF ONE-DIMENSIONAL ORGANIC CONDUCTORS

N. ARA-KATO, M. HARA, H. SASABE and W. KNOLL
Frontier Research Program, RIKEN, Wako, Saitama 351-01, Japan

Abstract On the basis of highly reproducible scanning tunneling microscopy (STM) images of the tetrathiafulvalene-tetracyanoquinodimethane (TTF-TCNQ) surface with atomic resolution, a new interpretation for such STM images from the viewpoint of the relative phase difference of the molecular orbital in each organic molecule is presented. The interpretation is based on the interference effect on tunneling because of the short tip-sample distance.

INTRODUCTION

The first scanning tunneling microscopy (STM)[1] image for organic materials with atomic resolution was obtained for the crystalline surface of an organic conductor, tetrathiafulvalene-tetracyanoquinodimethane (TTF-TCNQ), by Sleator and Tycko (ST).[2] They reported that its STM images well reflect spatial distribution of the absolute value of the highest occupied molecular orbital (HOMO) of a TTF molecule and the lowest unoccupied molecular orbital (LUMO) of a TCNQ molecule, which is expected by the STM theory proposed by Tersoff and Hamann (TH theory).[3]

Several STM studies of TTF-TCNQ films formed by vacuum deposition have been reported by STM because of its interesting physical properties.[4] In numerous such studies, it has been realized that there exist two types of the molecular images, an acute-angle chevron type and an obtuse-angle chevron type, and the former has similar features to the images of TTF-TCNQ crystals.[2] Here, we report the details of the two types of the STM images and present a new interpretation for such images of TTF-TCNQ by considering the relative phase difference of TTF HOMO or TCNQ LUMO.

EXPERIMENTAL

TTF-TCNQ complex was prepared by mixing TTF and TCNQ in acetonitrile solution and leaving the mixture at ambient temperature for one week to allow the solvent to evaporate slowly. Mica substrates were cleaved in air and heated at 100 °C for one hour

under a vacuum of 3 x 10^{-4} Pa for cleaning. TTF-TCNQ molecules were deposited on the mica substrate at room temperature and in high vacuum of 1 x 10^{-4} Pa. The deposition rate was 10 nm/min and the thickness of the films was about 100 nm. STM imaging was carried out in air at room temperature with 80% Pt - 20% Ir tips in a constant height mode. The STM system used in this study was a commercial NanoScope II (Digital Instruments, Inc., Santa Barbara, CA, USA).

RESULTS AND DISCUSSION

TTF-TCNQ crystal is monoclinic with lattice constants : a = 1.2298 nm, b = 0.3819 nm, c = 1.8468 nm, β = 104.46°. Figure 1(a) shows molecular arrangement of TTF-TCNQ crystal, as determined by X-ray diffraction,[5] projected onto the *ab*-plane. Since the molecules form homologous columns along the b-axis and molecular orbitals between adjacent molecules in each column overlap along this direction, the crystal has high one-dimensional electronic conductivity along the b-axis. TTF and TCNQ molecular planes are set at an angle of 58.5° to one another. They are oppositely directed by 24.5° and 34.0°, respectively, relative to the axis $c^* = a \times b$, as shown in Fig.1(b).

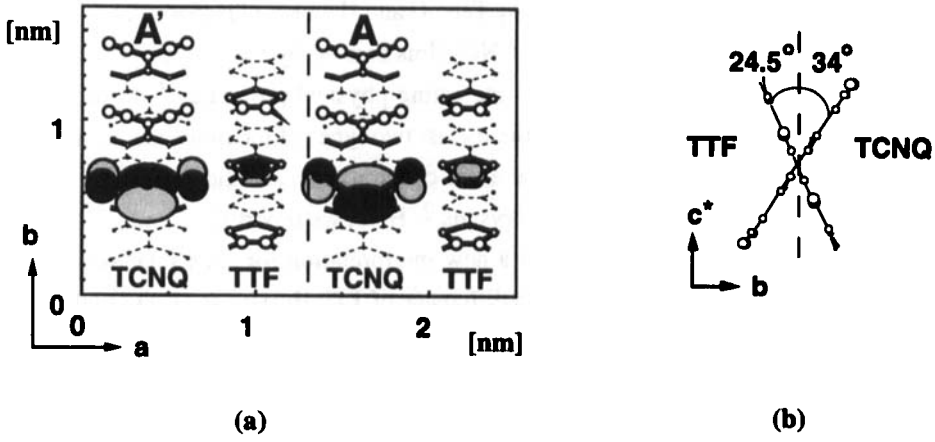

FIGURE 1 (a) Molecular arrangement of TTF-TCNQ projected onto *ab*-plane (b) Angular relation between TTF and TCNQ molecules.

Figure 2 shows a typical TTF-TCNQ image obtained at sample bias voltage of 4.9 mV and tunnel current of 0.42 nA. Molecular images indicated by A and B have characteristics similar to those of the crystal obtained by ST.[2] According to their assignment based on computer simulation, A and B are TCNQ and TTF, respectively. However, TCNQ images indicated by A' are quite different from A. Two types of TCNQ molecular images alternate every one or two rows. The main differences of the TCNQ images A' compared to the images A can be summarized as follows:

(1) The chevron pattern of the TCNQ triplet A' is rotated 180 degrees.
(2) The triangular angle of the chevron pattern of the triplet A' is less acute.
(3) The surrounding outer balls are brighter than those of A.

In numerous STM studies, we have found no significant evidence of STM images other than types A and A'.

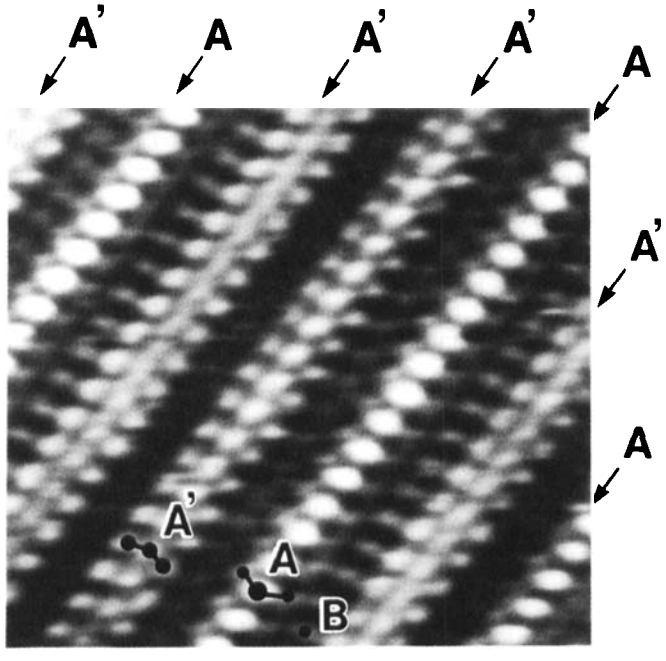

FIGURE 2 Typical STM image of TTF-TCNQ

In a previous report,[6] these differences in the STM images were explained by differences of the actual structures between columns including A and A'. Namely, molecular planes were thought to be tilted in opposite directions and have different tilt

angles between A and A'. However, we have found that these two types of TCNQ images cannot be reproduced in simulations by changing the tilt angle of the molecules.[7]

The interpretation of the STM images under the assumption that the differences in the relative phases have appeared in the images is presented here. Figure 3 shows the spatial distribution of TCNQ LUMO projected on *ab*-plane showing for the differences of its relative phase explicitly. The spatial distribution of TCNQ LUMO are schematically superimposed on the molecules. Characteristics of the TCNQ image of Fig. 2 are well explained as follows:

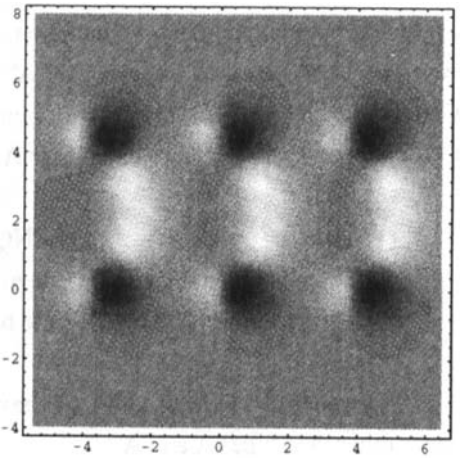

FIGURE 3 Simulated TCNQ image

(1) The angle of chevron pattern of TCNQ triplet A' is rotated 180 degrees and is less acute, similar to the actual TCNQ image.

(2) It can be interpreted that the surrounding outer balls of TCNQ triplet A' are brighter than those of TCNQ triplet A because of the shorter tunneling distance from the tip. This is also consistent with Fig. 1(a).

Also, the angle of the chevron pattern of TCNQ triplet A shown in Fig. 1(a), is as sharp as the actual TCNQ image and ST's image. From these results, it is clear that the characteristic features seen in the image can be explained well by introducing the relative orbital phases to STM imaging.

How the differences of relative phases of the molecular orbitals appear in STM images? The only possibility that the difference of relative phase of the molecular orbitals appear in STM images is the interference effect between a tip and a sample. In recent studies by computer simulation the tip-sample distance was evaluated to be less than 3Å.[8] In such a short tip-sample distance the interference effect between a tip and a sample can not be ignored on tunneling.

First we consider using a simple model which is composed of two identical isolated potential wells with energetically discrete states at a large distances. When the wells are brought closer together, their interaction leads to a splitting of each energy state. The wavefunctions for these states for each well can interfere constructively or destructively depending on their relative phases at a tunneling gap. This corresponds to

the bonding and antibonding states in a diatomic molecule. Since each electron interferes only with itself, as recently demonstrated in a two-slit experiment by Tonomura *et al.*,[9] each electron overlaps in-phase or out-of-phase at the gap independently of other electrons in many-electron systems. Therefore, we introduce such a splitting of energy to a tip-sample system in STM.

According to the WKB (Wentzel-Kramers-Brillouin) approximation, tunneling probability T of an electron for a whole system is expressed as follows;[10]

$$T \approx \exp\left(-\frac{2}{\hbar}\int_0^d \sqrt{2m\left(V(x)-E\right)}\,dx\right) \qquad (1)$$

where $V(x)$ is a barrier height, E is an energy of the electron, $\hbar = h / 2\pi$ (h is Planck constant) and m is a mass of the electron. d is a width of tunneling barrier at the energy E. If we know the energy of an electron for a whole system, we can estimate the tunneling probability according to equation (1).

Since the scan rate of the tip in the STM measurement is slow compared to the response time of the electron, the adiabatic approximation in the tip-sample system holds during a measurement. Since crystal orbitals in the conduction bands are approximately represented as linear combinations of the TTF HOMO or the TCNQ LUMO, the difference of the relative phase of each molecular orbital is preserved in each crystal orbital.

The energy of the new wavefunction made up from the tip-side and sample-side wavefunctions changes depending both on the absolute value and the sign of the overlap integral. This change of energy ΔE is equivalent to a resonance energy in quantum chemistry.[11] We consider that the energy changes to $E \pm \Delta E$ in the equation (1) according to in-phase or out-of-phase overlapping between the tip-side and sample-side wavefunctions. Thus, we obtain the tunneling probability for the new wavefunction as follows;

$$T \approx \exp\left(-\frac{2}{\hbar}\int_0^d \sqrt{2m\left(V(x)-(E\pm\Delta E)\right)}\,dx\right) \qquad (2)$$

The tunneling probability changes depending both on the absolute value and the sign of the overlap integral according to equation (2). In this sense, there exists a clear difference in tunneling probability between in-phase and out-of-phase overlappings.

Consequently, the characteristic differences in the STM images of TTF-TCNQ can be attributed to the changes of the tunneling probability with different phase overlappings.

CONCLUSION

Characteristics of STM images of TTF-TCNQ are very well explained by the interpretation that the difference of relative phase of TTF HOMO and TCNQ LUMO appear in the images. This originates from the interference effect between a tip and a sample.

ACKNOWLEDGMENT

The authors would like to express their gratitude to Prof. A. Kawazu of the University of Tokyo for his suggestion to the experimental studies. The authors would like to acknowledge to the Computer Center at The Institute of Physical and Chemical Research (RIKEN).

REFERENCES

1. G. Binnig, H. Rohrer, Ch. Gerber and E. Weibel, Phys. Rev. Lett. 49 (1982) 57 ; G. Binnig, H. Rohrer, Ch. Gerber and E. Weibel, Phys. Rev. Lett. 50 (1983) 120
2. T. Sleator and R. Tycko, Phys. Rev. Lett. 60 (1988) 1418
3. J. Tersoff and D. R. Hamann, Phys. Rev. Lett. 50 (1983) 1993 ; J. Tersoff and D. R. Hamann, Phys. Rev. B31 (1985) 805
4. A. Kawazu, N. Ara and M. Yoshimura,"Scanning Tunneling Microscopy of Organic Conductors" in *The Structure of Surfaces III* edited by S.Y. Tong, M. A. Van Hove, K. Takayanagi and X. D. Xie (Springer-Verlag,Berlin,1991) 214 ; N.Ara-Kato, K.Yase, H.shigekawa, M.Yoshimura and A.Kawazu, Synthetic Metals 70 (1995) 1245 ; N.Ara, H.Sigekawa, K.Yase, M.Yoshimura and A. Kawazu, App.Phys.Lett. 66 (1995) 3278
5. T. J. Kistenmacher, T. E. Phillips and D. O. Cowan, Acta. Crystallogr. B30 (1974) 793.
6. N. Ara, H. Sigekawa, K. Yase, M. Yoshimura and A. Kawazu, App.Phys.Lett. 66 (1995) 3278
7. N. Ara-Kato, M. Hara, H. Sasabe and W. Knoll (to be submitted)
8. N. Ara-Kato, M. Hara, H. Sasabe and W. Knoll (to be submitted)
9. A. Tonomura, J. Endo, T. Matsuda, T. Kawasaki and H. Ezawa, Am. J. Phys. 57 (1989) 117
10. L. D. Landau and L. M. Lifshitz, *Quantum Mechanics* (Pergamon, Oxford, 1977)
11. L. Pauling, *The Nature of the Chemical Bond* (Cornell University Press, New York, 1977)